

Evaluation of iron transport from ferrous glycinate liposomes using Caco-2 cell model.

Ding Baomiao, Yi Xiangzhou, Li Li, Yang Hualin

College of Life Science, Yangtze University, Jingmi Road 266, Jingzhou Hubei 434025, China

Abstract

Background: Iron fortification of foods is currently a strategy employed to fight iron deficiency in countries. Liposomes were assumed to be a potential carrier of iron supplements.

Objective: The objective of this study was to investigate the iron transport from ferrous glycinate liposomes, and to estimate the effects of liposomal carriers, phytic acid, zinc and particle size on iron transport using Caco-2 cell models.

Methods: Caco-2 cells were cultured and seeded in DMEM medium. Minimum essential medium was added to the basolateral side. Iron liposome suspensions were added to the apical side of the transwell.

Results: The iron transport from ferrous glycinate liposomes was significantly higher than that from ferrous glycinate. In the presence of phytic acid or zinc ion, iron transport from ferrous glycinate liposomes and ferrous glycinate was evidently inhibited, and iron transport decreased with increasing phytic acid concentration. Iron transport was decreased with increase of particle size increasing of ferrous glycinate liposome.

Conclusion: Liposomes could behave as more than a simple carrier, and iron transport from liposomes could be implemented via a mechanism different from the regulated non-heme iron pathway.

Keywords: Ferrous glycinate liposomes, iron transport, phytic acid, particle size.

DOI: <https://dx.doi.org/10.4314/ahs.v17i3.37>

Cite as: Baomiao D, Xiangzhou Y, Li L, Hualin Y. Evaluation of iron transport from ferrous glycinate liposomes using Caco-2 cell model. *Afri Health Sci.* 2017;17(3): 933-941. <https://dx.doi.org/10.4314/ahs.v17i3.37>

Introduction

Iron deficiency is a common nutritional disorder problem worldwide¹. Insufficient dietary intake and low iron bio-availability in foods are usually the primary contributing causes of iron deficiency^{2,3}. Iron fortification of foods is currently a strategy employed to fight iron deficiency in countries⁴. Iron supplements utilized in food fortification should be readily bioavailable, stable and safe⁵. Liposomes are potential carriers^{6,7}, and the delivery systems have been used to increase iron absorption in certain food matrices such as dairy products⁸.

Most of traditional iron supplements could injure the mucosa of the gastrointestinal tract, and high iron intake could also lead to iron overload in some human being, which could result in cell toxicity and side effects such

as respiratory morbidities, nausea, abdominal discomfort, constipation, and an increased risk of infection. Compared with common iron supplements, iron liposomes can obviously increase the iron levels and haemoglobin concentrations in serum so as to alleviate the anemia^{9,10}. Liposomal iron did not aggravate the oxidative stress at the same time of increasing iron levels in serum. Moreover, iron liposomes are microvesicles and mostly nano-sized particles, they also have physical stability and gradual release properties. Furthermore, they have no toxicity and minimal side effects to the body than unencapsulated iron supplements^{7,8}.

The absorption of non-heme iron, such as ferrous sulphate, could be restrained by several factors. Phytic acid in diets based on cereals and legumes has been shown to inhibit iron absorption in humans and in cell culture models¹¹. It has also been proved that some divalent metal ions (such as Zn²⁺) decreased iron uptake¹². The core material bioavailability could be improved by liposomes⁸, and the delivery efficiencies of liposomes to core materials are significantly influenced by liposomal physico-

Corresponding author:

Ding Baomiao,
Yangtze University, College of Life Science
Email: bmding@yangtzeu.edu.cn

African Health Sciences @ 2017 Baomiao et al; licensee African Health Sciences. This is an Open Access article distributed under the terms of the Creative Commons Attribution License (<https://creativecommons.org/licenses/by/4.0/>), which permits unrestricted use, distribution, and reproduction in any medium, provided the original work is properly cited.

chemical properties, such as particle size¹³. However, the effects of these factors on the regulation of iron transport by liposomes are still obscure.

The Caco-2 cells, a human adenocarcinoma cell line, shows promise as a rapid and low-cost model to predict iron absorption from foods and iron fortificants^{14,15}. The model system has been applied numerous times to estimate relative iron bioavailability from varieties of staple food crops, commercial food products, and meals or specific food, etc^{15,16}. To further assess the regulation of liposomes, iron transport experiments with ferrous glycinate liposomes were performed using Caco-2 cell model.

Ferrous glycinate as an iron chelate has been microencapsulated using liposomes in previous work, and the pH stability of the iron supplement obviously increased^{17, 18}. The objective of the present study was to evaluate the regulation of iron transport by liposomes using Caco-2 cell model, and to provide information on the effects of known inhibitors of iron transport from ferrous glycinate liposomes (i.e. phytic acid and zinc), and to determine the effects of liposome particle size. Documentation of these results will be valuable to understand the regulation of liposomes on iron transport and to predict the iron availability of ferrous glycinate liposomes.

Material and methods

Materials

Egg phosphatidylcholine (EPC), cholesterol, Tween 80 and diethyl ether were purchased from Sinopharm Chemical Reagent Co., Ltd (Shanghai, China). Minimum essential medium (MEM medium), D-Hanks buffer, phytic acid and ZnCl₂ were obtained from Sigma-Aldrich Co., LLC (Shanghai, China). All chemicals were of reagent grade and used without further purification. Ferrous glycinate was synthesized according to CN Patent ZL200410065260.3.

Preparation of ferrous glycinate liposomes

Ferrous glycinate liposomes were prepared by reverse phase evaporation (REV) method¹⁹. Briefly, the lipid mixture, containing EPC (200 mg) and cholesterol (20 mg), was dissolved in 10 mL diethyl ether (organic phase). Ferrous glycinate (40 mg) was dissolved in 3 mL aqueous solution (phosphate buffer solution, PBS, 0.05 mol/L, pH6.8). The aqueous phase was added to the

organic phase, and then a homogeneous w/o emulsion was obtained by ultrasonication with a probe sonicator (VCX400, Sonics & Material, USA) with a sequence of 1 s on and 1 s off (sonication power 300 W) in an ice bath for 5 min. The w/o emulsion in a round bottom flask was evaporated using a rotary evaporator under reduced pressure at 40°C, and a gel was formed. Upon further rotary evaporation, the gel was broken, and then 10 mL PBS buffer (0.05 mol/L, pH6.8) containing 100 mg Tween 80 was added with gentle vortexing and the sample was sequentially evaporated for 30 min at 40°C. The residual diethyl ether was evacuated by nitrogen gas.

Procedures to purify ferrous glycinate liposomes and to control liposomal particle sizes

The purification and particle size control of ferrous glycinate liposomes was processed simultaneously. Firstly, liposomes were separated according to the particle size by Sephadex G-100 column (20 cm × 1 cm id), and the samples were eluted using 0.9% (w/v) NaCl solution, and the eluate was collected by test tubes per minute. Secondly, liposomes were extruded to adjust particle sizes using an ultrafiltration cell (Amicon stirred cell 8010, Millipore, USA) with a polycarbonate membrane (1.0, 0.6, 0.4, 0.2, and 0.1 μm pores). Samples were extruded through a membrane using N₂ gas, and extruded solution was collected. The obtained solution could be further extruded to reduce the particle size using a membrane with next smaller pore size. At last, the first step was repeated to eliminate free iron. Particle size and size distribution were measured by dynamic light scattering with a ZEN3600 Zetasizer nano instrument (Malvern Instrument, Worcs, UK).

Cell culture

Caco-2 cells were obtained from the American Type Culture Collection (Rockville, MD, USA) between passages 25 to 30. Cells were cultured in DMEM medium for 14 d, 10% fetal bovine serum (FBS), 4.5 g/L glucose, 2 mmol/L L-glutamine, 100 U/mL penicillin and 100 U/mL streptomycin; the medium was replaced every two days. Caco-2 cells were seeded in flasks and incubated at 37 °C, under a 5% CO₂ in air atmosphere. After one week, the cells were harvested and reseeded in 12-well transwell plates at a density of 5×10⁴ cells/cm², and incubated to reach 100% confluence at 37°C, under a 5% CO₂ in air atmosphere. Transepithelial electrical resistance

(TEER) was measured to check the integrity of Caco-2 cell monolayers. The transwells consisted of the apical chamber (which simulated the intestinal lumen) and the basal chamber (which would collect the bioavailable iron), which were separated by a polycarbonate membrane with 0.4 μm pores.

Iron transport in Caco-2 cells

The apical and basolateral surfaces of Caco-2 cells in the transwell were rinsed three times with D-Hanks buffer solution. Then, 500 μl of MEM medium (contained no added iron), previously warmed at 37°C, was added to the basolateral side. Iron transport was started by the addition of 300 μl (1, 10, 20 and 50 $\mu\text{mol/L}$ iron, containing predetermine amount of phytic acid or ZnCl_2) of iron liposomes or ferrous glycinate in D-Hanks buffer solution in the apical side of the transwell. Then, they were incubated for 120 min at 37°C, under 5% CO_2 . After incubation, the transport was stopped by washing the inserts three times with ice-cold 1 mmol/L EDTA in PBS buffer (0.01 mol/L, pH7.4). The basolateral side solution was recovered for the determination of the iron transported across Caco-2 cells.

Determination of iron

The iron concentration was measured according to the procedure described by Jorhem²⁰. Briefly, aliquots of the samples were disrupted to remove organic compounds and to release elemental iron thoroughly by ashing for 10 h at 450°C in a muffle furnace. The inorganic residues were dissolved in 1 mol/L HCl. The determination of iron was performed by graphite furnace atomic absorption spectrophotometry (AAS, Zeenit 700P, Analytik Jena AG, Germany) at 248.3 nm. The calibration curves were performed with standard solutions containing 0-6 $\mu\text{g/mL}$ of ferric chloride in 1% (V/V) nitric acid.

Data analysis and statistical evaluation

The iron transport was calculated based on the iron amount as determined by AAS and the surface area of the cell monolayer. The iron transport was calculated using the following equation:

$$\text{Iron transport (pmol/cm}^2\text{)} = \text{MA}_{\text{Fe}} / A$$

where MA_{Fe} is the amount of substance of iron in the basolateral side; A is the surface area of the cell monolayer. Statistical analysis of the data was performed using Matlab software (Version 7.11.0.584(R2010b), MathWorks, Inc. Natick, Massachusetts, USA). Differences in the amount of iron transport were compared using two-way ANOVA. The differences were considered significantly different if P values were less than or equal to 0.05. Variance within treatment groups is expressed as standard deviation (SD).

Results and discussion

Effect of incubation time on iron transport from ferrous glycinate liposomes

Iron transport across Caco-2 cells treated with increasing incubation time at four levels, 30, 60, 90, and 120 min, are shown in Figure 1. Iron transport of ferrous glycinate liposomes was in agreement with that of ferrous glycinate, which was time-dependent for the period of 120 min, and the iron tended to increase with increasing incubation time. Moreover, iron transport was increased with increasing of iron concentrations. The iron transport from ferrous glycinate liposomes was significantly higher than that from ferrous glycinate (two-way ANOVA; incubation time and iron sources, $F[1, 16]=9.38$, $p=0.0074$). Compared to ferrous glycinate, the relative iron transport of ferrous glycinate liposomes at 1, 10, and 50 $\mu\text{mol/L}$ and incubation for 120 min were 146.1%, 131.1%, and 128.9%, respectively, which indicated that the iron of ferrous glycinate liposomes across Caco-2 cells could be more efficient.

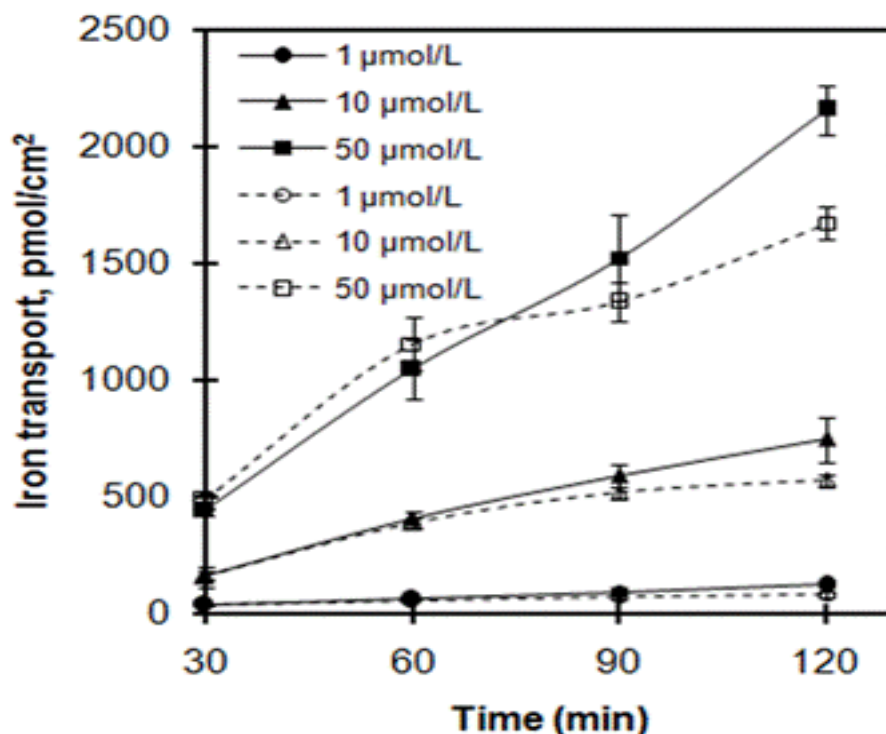


Figure 1: Effects of incubation time on iron transport across Caco-2 cells. Ferrous glycinate liposomes and ferrous glycinate are expressed in solid lineseries and dashed line series, respectively. Values are means \pm SD, n = 3.

Ferrous glycinate liposomes demonstrated higher iron transport than that from ferrous glycinate at the same iron level. The difference in the values of iron transport between the two iron sources was not so apparently in the initial phase or at low iron concentration, whereas the iron transport from ferrous glycinate liposomes was obvious higher than that from ferrous glycinate at the ultimate stage and at high concentration. The higher iron transport of ferrous glycinate liposomes could result from the protection of ferrous glycinate by liposomal vesicles¹⁸. The lipophile of liposomes was higher than that of ferrous glycinate, so the affinity between ferrous glycinate and cells could be enhanced by the iron encapsulated in liposomes^{21,22}. In addition, particle sizes of ferrous glycinate liposomes were nano-scale, so the liposomes could behave in nanoparticle effects²³.

Effects of phytic acid on iron transport from ferrous glycinate liposomes

Iron bioavailability was decreased by many inhibitors in the daily diet. Phytic acid extensively exists in vegetable food, such as cereals, beans, and it is a strong inhibitor

of non-heme iron transport^{24,25}. Figure 2 documented the iron transport in response to increasing concentrations of phytic acid. In the presence of phytic acid, iron transport from ferrous glycinate liposomes and ferrous glycinate was evidently inhibited, and iron transport decreased with increasing of phytic acid concentration. However, two-way ANOVA results (phytic acid concentration and iron sources, $F[1, 20]=575.15$, $p<0.001$) showed that effects of phytic acid on iron transport from ferrous glycinate liposomes and ferrous glycinate were significantly different. Compared with ferrous glycinate, iron transport from ferrous glycinate liposomes was less inhibited by phytic acid. For example, at the iron concentration of 50 $\mu\text{mol/L}$, the iron transport at phytic acid concentration of 100, 200, 500, and 1000 $\mu\text{mol/L}$ were decreased by 3.0%, 4.6%, 7.4%, and 14.0% for ferrous glycinate liposomes and by 8.0%, 16.5%, 27.0%, and 45.2% for ferrous glycinate, respectively. Compared to ferrous glycinate, the relative iron transport of ferrous glycinate liposomes at 1, 10, 20, and 50 $\mu\text{mol/L}$ at phytic acid concentration of 100 $\mu\text{mol/L}$ were 213.7%, 149.4%, 136.2%, and 135.9%, respectively.

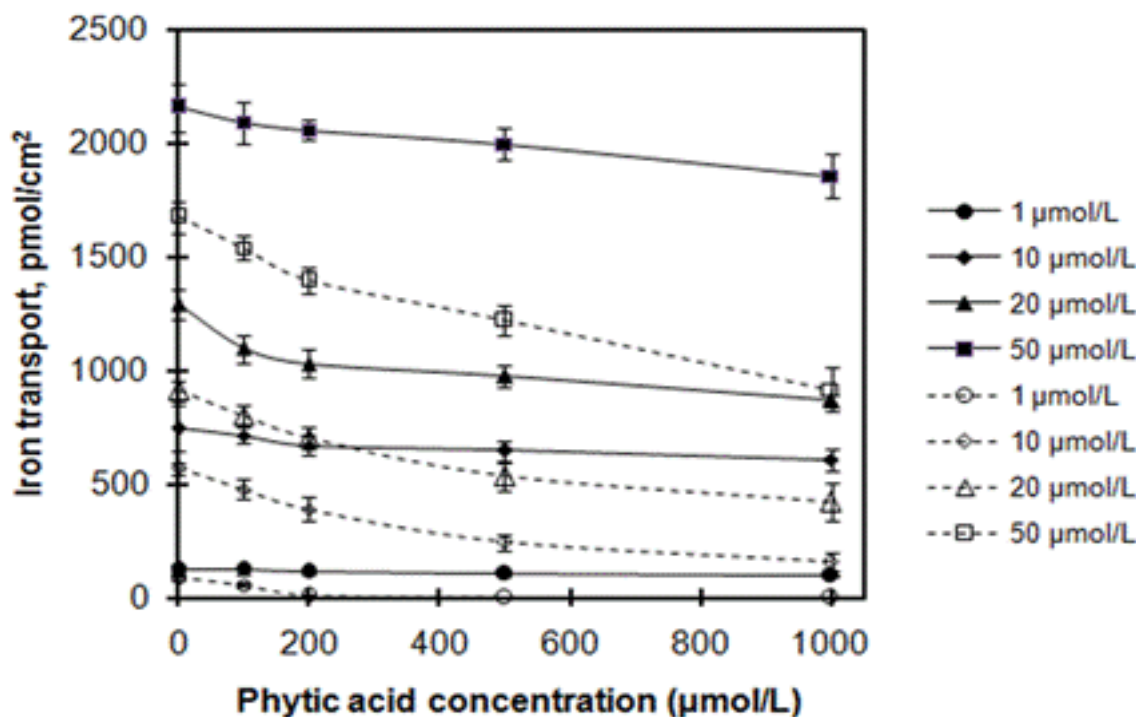


Figure 2: Effects of phytic acid on iron transport across Caco-2 cells. Ferrous glycinate liposomes and ferrous glycinate are expressed in solid line series and dashed line series, respectively. Values are means \pm SD, n = 3.

Phytic acid has proved to be a stubborn inhibitor of iron absorption in humans, which widely exists in cereals and soybeans^{11,26}. The compound is prone to chelate divalent metal ions and to form insoluble and indigestible chelate complex, which would result in the loss of iron absorption²⁷. The results of Figure 2 exhibited that iron transport from ferrous glycinate was seriously decreased by phytic acid. However, iron transport from ferrous glycinate liposomes was less inhibited by the organic acid. The higher iron transport from ferrous glycinate liposomes may be due to the encapsulation of ferrous glycinate in liposomes, and the iron was protected from phytic acid by the phospholipids bilayer membrane, which prevented the formation of insoluble phytate-iron complex²⁸.

Effects of Zinc ion on iron transport from ferrous glycinate liposomes

The interactions of iron and zinc in foods represent critical nutrition issues. The effects of zinc on iron transport are summarized in Figure 3. The addition of zinc at con-

centrations of 0, 10, 50, 100, and 300 $\mu\text{mol/L}$ decreased iron transport, which was decreased with increasing of zinc concentration. However, judging from the two-way ANOVA results (ZnC_{12} concentration and iron sources, $F[1, 20]=448.64, p<0.001$), there were significantly different effects of ZnC_{12} on iron transport from ferrous glycinate liposomes and ferrous glycinate. Compared with ferrous glycinate, iron transport from ferrous glycinate liposomes was less affected by zinc. For instance, at the iron concentration of 50 $\mu\text{mol/L}$, iron transport at zinc concentration of 10, 50, 100 and 300 $\mu\text{mol/L}$ were decreased by 4.7%, 9.6%, 14.1%, and 20.9% for ferrous glycinate liposomes and by 9.7%, 28.7%, 48.0%, and 57.2% for ferrous glycinate, respectively. Compared to ferrous glycinate, the relative iron transport of ferrous glycinate liposomes at 1, 10, 20, and 50 $\mu\text{mol/L}$ at the zinc concentration of 50 $\mu\text{mol/L}$ were about 10.3-fold, 2.0-fold, 2.2-fold, and 1.6-fold, respectively. The results implied that liposomes could improve the anti-inhibition of iron.

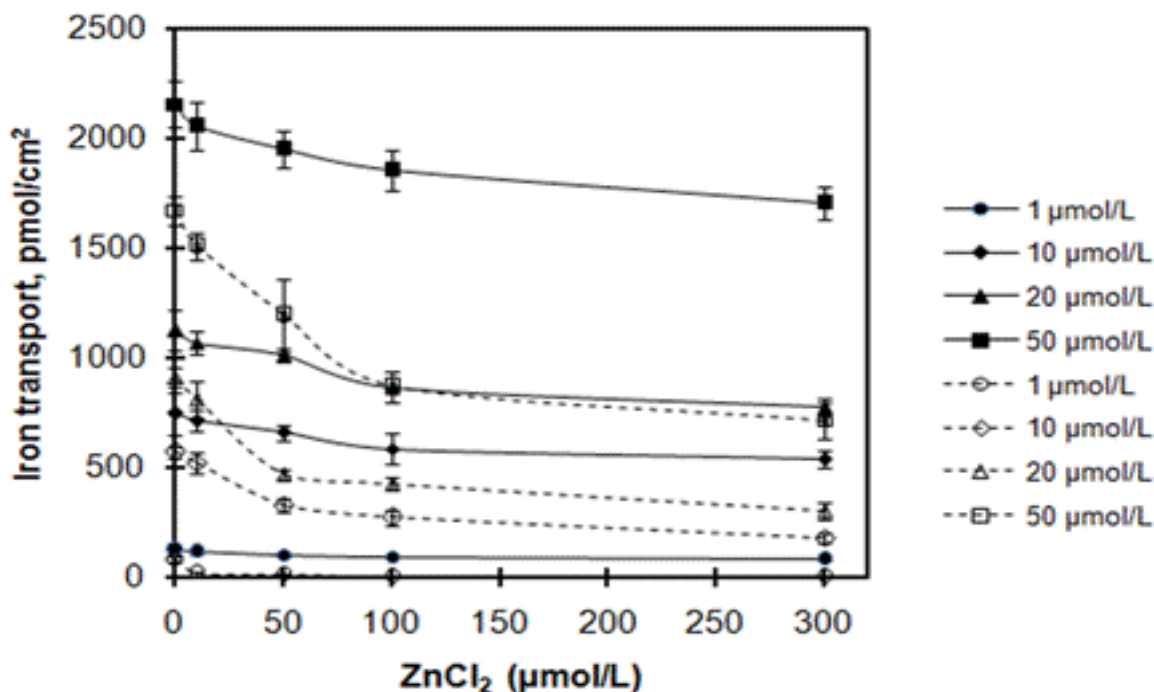


Figure 3: Effects of ZnCl₂ on iron transport across Caco-2 cells. Ferrous glycinate liposomes and ferrous glycinate are expressed in solid line series and dashed line series, respectively. Values are means ± SD, n = 3.

Plenty of literature evidenced that the interaction of iron and zinc in foods was antagonistic effect, which would cause the reduction in bioavailability of the two mineral elements^{29,30}. Espinoza et al. and Iyengar et al. reported that divalent metal transporter 1 (DMT1) and/or Zip14 (Zrt- and Irt-like protein 14) were the probable iron and zinc interaction site^{31,32}. Representative results from Figure 3 indicated that iron transport from ferrous glycinate was sharply decreased with increasing of zinc concentration. It could be inferred that the antagonism between iron and zinc has not been eliminated. Compared to ferrous glycinate, the higher iron transport from ferrous glycinate liposomes might be attributed to the fact that the iron was encapsulated in liposomal vesicles. Liposomes could be delivered via membrane fusion, diffusion or phagocytosis^{33,34}, so iron was more efficiently transported. It could be speculated that ferrous glycinate loaded in phospholipid vesicles could be transported by liposomes rather than DMT1 protein. It was conceivable that ferrous glycinate liposomes could be absorbed through endocytic pathway, and the antagonistic effect between iron and zinc was abated. Pereira et al. affirmed that iron encapsulated in nanoparticles was utilized following acquisition by endocytic uptake³⁵. Niu et al. reported that liposomes were likely to be absorbed intact via the M-cell

or the epithelia pathways¹³. However, the bilayer membrane of liposomes could be destroyed by divalent metal cation-induced destabilization³⁶. And it could lead to leakage of iron from ferrous glycinate liposomes, and the iron transport decreased.

Effect of particle size on iron transport from ferrous glycinate liposomes

Iron transport of ferrous glycinate liposomes at five particle sizes, 70, 100, 150, 300, and 500 nm were assessed (Figure 4). As shown in Figure 4, iron transport was decreased with particle size increasing of ferrous glycinate liposome at selected iron concentrations. A two-way ANOVA was performed to determine the statistical significance of particle size and iron concentration as factors. Significant effects of particle size and the interaction between particle size and iron concentration interactions were observed (one-way ANOVA, particle size, $F[4, 40]=84.94, p<0.001$; two-way ANOVA, particle size and iron concentration, $F[12, 40]=4.81, p<0.001$). liposomes with smaller particle size of about 70 nm exhibited evidently higher iron transport than liposomes with bigger particle size of 300 and 500 nm (two-way ANOVA; $p<0.001$ in both cases). Liposomes with particle size of 300 and 500 nm exhibited lower iron transport. The iron transport was not sig-

nificantly different ($p > 0.05$) between these two particle sizes. An example of the effects of particle sizes was the decrease of the iron transport with particle size increasing at the iron concentration of $50 \mu\text{mol/L}$ (ANOVA; $F[4, 10] = 29.91$; $p < 0.001$), and compared to that of 70

nm the iron transport was decreased by 11.4%, 20.1%, 26.9%, 33.3% for ferrous glycinate liposomes with particle sizes of 100, 150, 300, and 500 nm, respectively. The obvious size-dependent behavior indicated some kind of size-dependent recognition and internalization of ferrous glycinate liposomes.

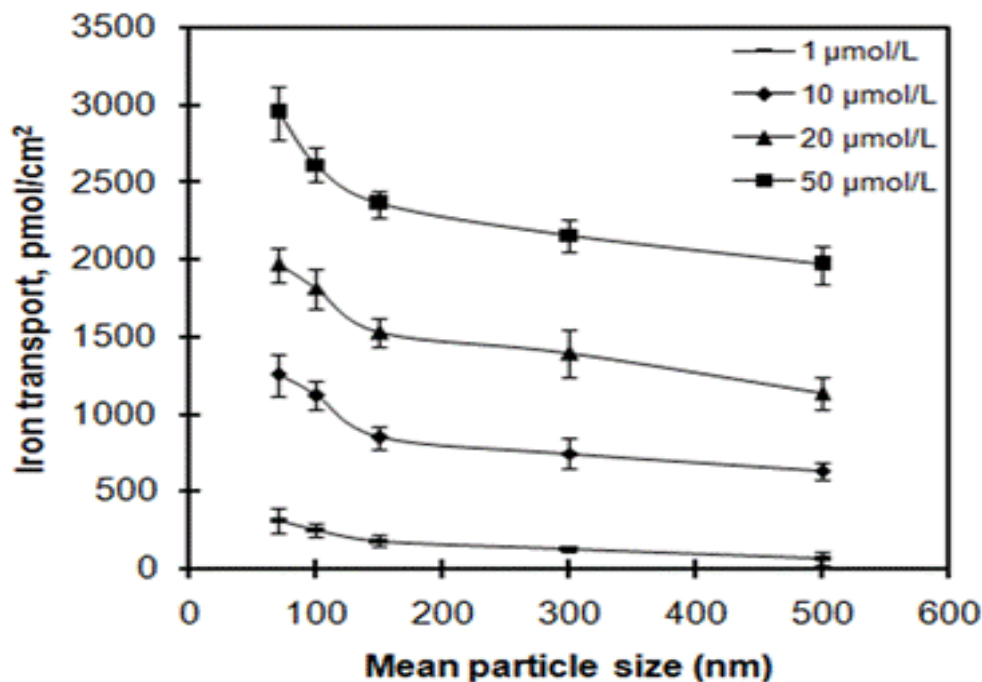


Figure 4: Effects of mean particle size on iron transport across Caco-2 cells. Values are means \pm SD, $n = 3$.

It has been revealed that particle size plays a vital role in nanoparticle adhesion to and interaction with biological cells^{37,38}. Iron transport from ferrous glycinate liposomes was size-dependent, i.e. it increased with the decreasing of particle sizes (Figure 4). In the present study, these results were coincident with previous results in which core material bioavailability from liposomes increased with particle size decreasing^{37,39}. It was generally supposed that particles within the 100-200 nm size range could be internalized via the pathway of receptor-mediate endocytosis, while particles with larger sizes would be captured by phagocytosis³⁷. However, particles in the size range of approximately 2-100 nm could play an active role in mediating biological effects more than being carriers. Signaling processes essential for basic cell functions could be altered by the smaller particles³⁹. The exact absorption mechanisms of particles with different sizes need to be elucidated in further studies.

The iron transport offered as ferrous glycinate liposomes was evaluated using Caco-2 cells, as a model of human intestinal epithelia. The results from this study strongly suggest that iron from ferrous glycinate liposomes was transported more effectively than that from ferrous glycinate. The effects of some common inhibitors, such as phytic acid and zinc on, on iron transport from liposomes were obviously decreased, compared to ferrous glycinate. It may be ascribed to the protection of phospholipide bilayer membrane on ferrous glycinate from common inhibitors. The fact quite possibly meant that the transport pathway of iron encapsulated in liposomes was different from that of free-iron. Furthermore, the iron transport was regulated by the size of liposomes, and it decreased with particle size increasing. Liposomes with the sizes of less than 100 nm, among 100-200 nm, and larger than 200 nm could be taken up via different pathways, such as altering signaling processes essential for basic cell functions, receptor-mediate endocytosis, phagocytosis, rather than traditional absorption pathway.

Conclusion

Liposomes could behave as more than a simple carrier, and iron transport from liposomes could be implemented via a mechanism different from the regulated non-heme iron pathway.

Acknowledgment

The research was supported by the National Natural Science Foundation of China (31401477).

Conflict of interest

The authors declare no conflict of interest.

References

1. Tang N, Zhu Y, Zhuang H. Antioxidant and anti-anemia activity of heme iron obtained from bovine hemoglobin. *Food Science and Biotechnology*. 2015;24:635-642.
2. Collings R, Harvey LJ, Hooper L, Hurst R, Brown TJ, Ansett J, King M, Fairweather-Tait SJ. The absorption of iron from whole diets: a systematic review. *The American Journal of Clinical Nutrition*. 2013;98:65-81.
3. Abbaspour N, Hurrell R, Kelishadi R. Review on iron and its importance for human health. *Journal of Research in Medical Sciences*. 2014;19:164-174.
4. Salgueiro MJ, Zubillaga M, Lysionek A, Caro R, Weill R, Boccio J. Fortification strategies to combat zinc and iron deficiency. *Nutrition reviews*. 2002;60:52-58.
5. Quintaes KD, Barbera R, Cilla A. Iron bioavailability in iron fortified cereal foods: the contribution of in vitro studies. *Critical Reviews in Food Science & Nutrition*. 2015. doi:10.1080/10408398.2013.866543
6. Tan C, Feng B, Zhang X, Xia W, Xia S. Biopolymer-coated liposomes by electrostatic adsorption of chitosan (chitosomes) as novel delivery systems for carotenoids. *Food hydrocolloids*. 2016;52:774-784.
7. Tan C, Zhang Y, Abbas S, Feng B, Zhang X, Xia S. Modulation of the carotenoid bioaccessibility through liposomal encapsulation. *Colloids and surfaces B: biointerfaces*. 2014;123:692-700.
8. Khanniri E, Bagheripoor-Fallah N, Sohrabvandi S, Mortazavian AM, Khosravi-Darani K, Mohammad R. Application of liposomes in some dairy products. *Critical Reviews in Food Science & Nutrition*. 2016;56:484-493.
9. Yuan L, Geng L, Ge L, Yu P, Duan X, Chen J, Chang Y. Effect of iron liposomes on anemia of inflammation. *International Journal of Pharmaceutics*. 2013;454:82-89.
10. Pisani A, Riccio E, Sabbatini M, Andreucci M, Del Rio A, Visciano B. Effect of oral liposomal iron versus intravenous iron for treatment of iron deficiency anaemia in CKD patients: a randomized trial. *Nephrology dialysis transplantation*. 2015;30:645-652.
11. Petry N, Egli I, Gahutu JB, Tugirimana PL, Boy E, Hurrell R. Phytic acid concentration influences iron bioavailability from biofortified beans in Rwandese women with low iron status. *Journal of nutrition*. 2014;144:1681-1687.
12. Olivares M, Castro C, Pizarro F, de Romana DL. Effect of increasing levels of zinc fortificant on the iron absorption of bread co-fortified with iron and zinc consumed with a black tea. *Biological Trace Element Research*. 2013;154:321-325.
13. Niu M, Lu Y, Hovgaard L, Guan P, Tan Y, Lian R, Qi J, Wu W. Hypoglycemic activity and oral bioavailability of insulin-loaded liposomes containing bile salts in rats: the effect of cholate type, particle size and administered dose. *European Journal of Pharmaceutics and Biopharmaceutics*. 2012;81:265-272.
14. Bodnar AL, Proulx AK, Scott MP, Beavers A, Reddy MB. Iron bioavailability of maize hemoglobin in a Caco-2 cell culture model. *Journal of agricultural and food chemistry*. 2013;61:7349-7356.
15. Eagling T, Wawer AA, Shewry PR, Zhao FJ, Fairweather-Tait SJ. Iron bioavailability in two commercial cultivars of wheat: comparison between wholegrain and white flour and the effects of nicotianamine and 2'-deoxymugineic acid on iron uptake into Caco-2 cells. *Journal of agricultural and food chemistry*. 2014;62: 10320-10325.
16. Pullakhandam R, Nair KM, Pamini H, Punjal R. Bioavailability of iron and zinc from multiple micronutrient fortified beverage premixes in Caco-2 cell model. *Journal of food science*. 2011;76: H38-H42.
17. Ding B, Xia S, Hayat K, Zhang X. Preparation and pH stability of ferrous glycinate liposomes. *Journal of agricultural and food chemistry*. 2009;57:2938-2944.
18. Ding BM, Zhang XM, Hayat K, Xia SQ, Jia CS, Xie MY, Liu CM. Preparation, characterization and the stability of ferrous glycinate nanoliposomes. *Journal of food engineering*. 2011;102:202-208.
19. Szoka F Jr, Papahadjopoulos D. Procedure for preparation of liposomes with large internal aqueous space and high capture by reverse-phase evaporation. *Proceedings of the national academy of sciences*. 1978;75:4194-4198.
20. Jorhem L. Determination of metals in foodstuffs by atomic absorption spectrophotometry after dry ashing:

- NMKL interlaboratory study of lead, cadmium, zinc, copper, iron, chromium, and nickel. *Journal of AOAC international*. 1993;76:798-813.
21. Danelian E, Karlén A, Karlsson R, Winiwarter S, Hansson A, Löfås S, Lennernäs H, Hämäläinen MD. SPR biosensor studies of the direct interaction between 27 drugs and a liposome surface: correlation with fraction absorbed in humans. *Journal of medicinal chemistry*. 2000;43:2083-2086.
 22. Miller CR, Bondurant B, McLean SD, McGovern KA, O'Brien DF. Liposome-cell interactions in vitro: effect of liposome surface charge on the binding and endocytosis of conventional and sterically stabilized liposomes. *Biochemistry*. 1998;37:12875-12883.
 23. Albanese A, Tang PS, Chan WC. The effect of nanoparticle size, shape, and surface chemistry on biological systems. *Annual review of biomedical engineering*. 2012;14:1-16.
 24. Baek JE, Lee EJ, Koh BK. The effects of germination, fermentation, and fermentation additives on the phytate content of rice flour. *Food science and biotechnology*. 2014;23:1447-1451.
 25. Wang X, Yang R, Jin X, Zhou Y, Han Y, Gu Z. Distribution of phytic acid and associated catabolic enzymes in soybean sprouts and indoleacetic acid promotion of Zn, Fe, and Ca bioavailability. *Food science and biotechnology*. 2015;24:2161-2167.
 26. Armah SM, Boy E, Chen D, Candal P, Reddy MB. Regular consumption of a high-phytate diet reduces the inhibitory effect of phytate on nonheme-iron absorption in women with suboptimal iron stores. *Journal of nutrition*. 2015;145:1735-1739.
 27. Andrews M, Briones L, Jaramillo A, Pizarro F, Arredondo M. Effect of calcium, tannic acid, phytic acid and pectin over iron uptake in an in vitro Caco-2 cell model. *Biological trace element research*. 2014;158:122-127.
 28. Akbarzadeh A, Rezaei-Sadabady R, Davaran S, Joo SW, Zarghami N, Hanifehpour Y, Samiei M, Kouhi M, Nejati-Koshki K. Liposome: classification, preparation, and applications. *Nanoscale research letters*. 2013;8:102.
 29. De Brito NJ, Rocha ED, de Araujo Silva A, Costa JB, Franca MC, das Gracas Almeida M, Brandao-Neto J. Oral zinc supplementation decreases the serum iron concentration in healthy schoolchildren: a pilot study. *Nutrients*. 2014;6:3460-3473.
 30. Zaman K, McArthur JO, Abboud MN, Ahmad ZI, Garg ML, Petocz P, Samman S. Iron supplementation decreases plasma zinc but has no effect on plasma fatty acids in non-anemic women. *Nutrition research*. 2013;33:272-278.
 31. Espinoza A, Le Blanc S, Olivares M, Pizarro F, Ruz M, Arredondo M. Iron, copper, and zinc transport: inhibition of divalent metal transporter 1 (DMT1) and human copper transporter 1 (hCTR1) by shRNA. *Biological trace element research*. 2012;146:281-286.
 32. Iyengar V, Pullakhandam R, Nair KM. Coordinate expression and localization of iron and zinc transporters explain iron-zinc interactions during uptake in Caco-2 cells: implications for iron uptake at the enterocyte. *The Journal of nutritional biochemistry*. 2012;23:1146-54.
 33. Lo YL. Phospholipids as multidrug resistance modulators of the transport of epirubicin in human intestinal epithelial Caco-2 cell layers and everted gut sacs of rats. *Biochemical pharmacology*. 2000;60:1381-1390.
 34. Lo Y, Liu F, Cheng J. Effect of PSC 833 liposomes and intralipid on the transport of epirubicin in Caco-2 cells and rat intestines. *Journal of controlled release*. 2001;76:1-10.
 35. Pereira DI, Mergler BI, Faria N, Bruggaber SF, Aslam MF, Poots LK, Prassmayer L, Lonnerdal B, Brown AP, Powell JJ. Caco-2 cell acquisition of dietary iron(III) invokes a nanoparticulate endocytic pathway. *PLoS ONE*. 2013;8:e81250.
 36. Deleers M, Servais JP, Wulfert E. Synergistic effects of micromolar concentrations of Zn²⁺ and Ca²⁺ on membrane fusion. *Biochemical and biophysical research communications*. 1986;37:101-107.
 37. Win KY, Feng SS. Effects of particle size and surface coating on cellular uptake of polymeric nanoparticles for oral delivery of anticancer drugs. *Biomaterials*. 2005;26:2713-2722.
 38. Verma A, Stellacci F. Effect of surface properties on nanoparticle-cell interactions. *Small*. 2010;6:12-21.
 39. Jiang W, Kim BY, Rutka JT, Chan WC. Nanoparticle-mediated cellular response is size-dependent. *Nature nanotechnology*. 2008;3:145-150.